ACS OMEGA

http://pubs.acs.org/journal/acsodf

Article

Synthesis and Photoreactivity of 7-Nitroindoline-*S*-thiocarbamates

Philip T. Baily,[‖] H. Patricio Del Castillo,[‖] Irodiel Vinales, Juan E. M. Urbay, Aurelio Paez, Matthew R. Weaver, Roberto Iturralde, Igor L. Estevao, Sohan R. Jankuru, Igor C. Almeida, Chunqiang Li,* Carl W. Dirk,* and Katja Michael*

Cite This: *ACS Omega* 2023, 8, 9486−9498

Read Online

ACCESS | Metrics & More | Article Recommendations | Supporting Information

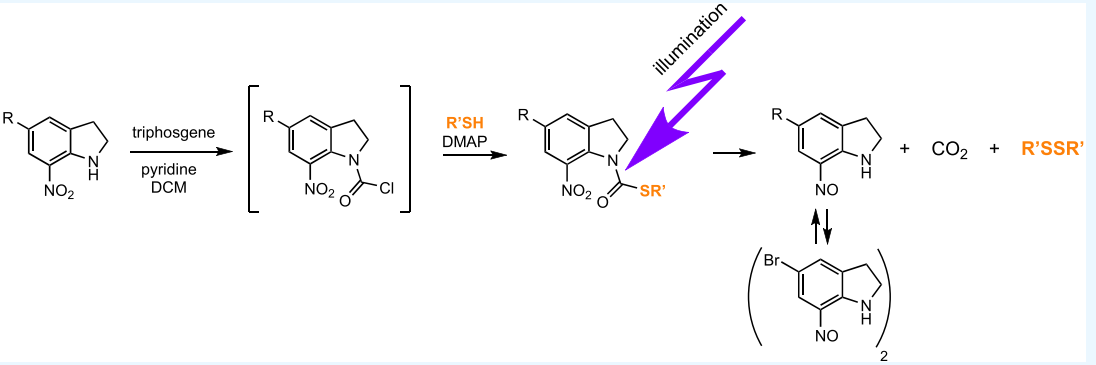

ABSTRACT: The photolytic properties of *N*-acyl-7-nitroindolines make these compounds attractive as photocleavable protecting groups and "caged" compounds for the light-induced release ("uncaging") of biologically active compounds and as acylating reagents under neutral conditions. However, the synthesis of *N*-acyl-7-nitroindolines usually requires multiple steps, and the direct acylation of 7-nitroindolines can be quite challenging. 7-Nitroindolines with other types of *N*-carbonyl-containing groups may also be photoreactive and could potentially be better accessible. Here we demonstrate the short and efficient synthesis of 5-bromo-7-nitroindoline-*S*-thiocarbamates, a new class of photoreactive compounds, and the study of some of their photochemical and photophysical properties. Using 5-bromo-7-nitroindoline-*S*-ethylthiocarbamate as a model compound, we show that it can undergo one-photon and two-photon photolysis at 350 and 710 nm, respectively. Our experimental data and quantum chemistry calculations support a photolysis pathway that differs from photolysis pathways previously reported for *N*-acyl-7-nitroindolines. The photolysis with 350 nm light results in 5-bromo-7-nitrosoindoline, which is in equilibrium with its dimeric form(s), as supported by experiment and theory. This study expands the scope of photoreactive 7-nitroindoline derivatives and informs the development of novel photocleavable compounds.

INTRODUCTION

In 1976, Amit and Patchornik reported the development of light-sensitive amides synthesized by acylation of 7-nitroindolines.[1] These *N*-acyl-7-nitroindolines (**1**) are activated by near UV or indigo-colored light, generating highly reactive nitronic anhydride intermediates (**2**) that cannot be isolated (Scheme 1).[2] The nitronic anhydrides react further by two different pathways that are solvent-dependent: (a) they are capable of acylating nucleophiles such as water, amines, and alcohols in inert aprotic solvents producing carboxylic acids, amides, and esters, respectively, as well as 7-nitroindolines (**3**) by an addition−elimination reaction.[2,3] (b) Alternatively, in aqueous media, an ε-elimination followed by a tautomerization takes place, resulting in carboxylic acids and 7-nitrosoindoles (**4**).[2,3] Different mechanisms for the formation of the common nitronic anhydride precursor (**2**) have been proposed,[2,4−7] including an addition−elimination via a cyclic intermediate,[2] and a combined Norish type I and type II acyl migration from the indoline nitrogen to the neighboring nitro group.[7]

Several applications of *N*-acyl-7-nitroindolines have been described. For example, neuroactive amino acids that had been caged as *N*-acyl-7-nitroindolines were released ("uncaged") by one-photon as well as two-photon photolysis.[3,5,8−10] Amides of 5-bromo-7-nitroindoline (Bni) have been used as a photocleavable protecting group;[11] as a photoactivatable, *C*-terminal group in peptide fragment condensation;[12] in the photochemical synthesis of glycosylamino acids;[13,14] as well as the

Received: December 25, 2022
Accepted: January 25, 2023
Published: February 27, 2023

https://doi.org/10.1021/acsomega.2c08184
ACS Omega 2023, 8, 9486−9498

Scheme 1. Solvent-Dependent Photolysis Pathways for *N*-Acyl-7-nitroindolines

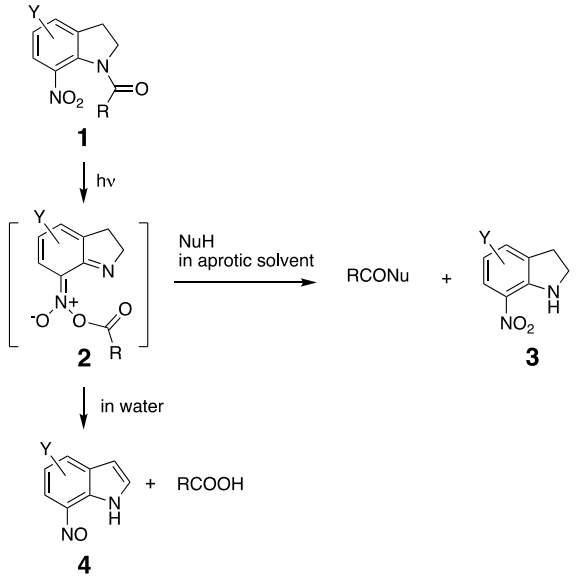

convergent synthesis of *N*-glycopeptides.[15] Amino acid building blocks with the 5,7-dinitroindoline (Dni) group at the *C*-terminus and a dimethyl-3,5-dimethoxybenzyloxycarbonyl (Ddz) group at the *N*-terminus were used for the all-photochemical synthesis of a pentapeptide in solution.[16] *N*-acyl-5,7-dinitroindolines have also been used for the photochemical acylation of alcohols under mild conditions.[17] An *N*-acyl-7-nitroindoline-based photolabile linker was developed for solid-phase synthesis and was used for the photoinduced release of linear and cyclic amides from the solid support by intra- and intermolecular transamidation.[18] We have synthesized a similar 7-nitroindoline-based linker suitable for solid-phase peptide synthesis, which proved useful for the photochemical synthesis of peptide thioesters and hydrazides.[19,20] Thin films of amino acid and peptide derivatives of 7-nitroindolines have also been used for micropatterning by two-photon photolysis using femtosecond laser light at 710 nm.[21,22]

Recently, nucleoside derivatives of *N*-acetyl-7-nitroindoline were incorporated into a DNA oligomer, and their photoreactivity within a DNA/RNA duplex was studied.[23] Remarkably, the opposite strand was acetylated in an aqueous reaction medium. Known photoreactive 7-nitroindolines with *N*-carbonyl-groups other than amides are carbamate and urea derivatives.[18,24] Upon illumination of Bni-based ureas and carbamates with UV light in CH_2Cl_2/dioxane/H_2O 5:10:1, amines and alcohols are released, respectively; however, the ureas reacted sluggishly.[24] Other 7-nitroindoline-based carbamates, that is, Fmoc, Cbz, and Boc derivatives of Dni, were used for the photochemical protection of amines as carbamates.[25]

Our interest in nitroindoline derivatives stems from the potential to generate new photocleavable compounds under mild, neutral conditions. One disadvantage of *N*-acyl-7-nitroindolines is that they cannot always be efficiently prepared. Their synthesis often involves many reaction steps from indole or indoline precursors, and the direct acylation of 7-nitroindonines can be challenging due to the poor nucleophilicity of the aromatic amine in the presence of at least one aromatic nitro group. This typically requires acid chlorides as acylating agents, which can be difficult to prepare or handle, especially when acid-sensitive moieties are present in the molecule. We were looking for an alternative photoreactive 7-nitroindoline derivative that is easily accessible and retains photocleavability. Inspired by the synthesis of nitroindoline ureas and carbamates using phosgene or triphosgene to generate an intermediate carbamoyl chloride,[18,24] our idea was to synthesize *S*-thiocarbamates of 7-nitroindolines from a 7-nitroindoline (**3**), triphosgene, and a thiol. To the best of our knowledge, nitroindoline-*S*-thiocarbamates have not been reported yet, and whether such compounds would be photoreactive was unknown.

Here, we demonstrate the highly efficient one-pot synthesis of three 7-nitroindoline-*S*-thiocarbamates and the study of some of their photochemical and photophysical properties. Specifically, the progression of their photolysis at 350 nm was monitored by UV−vis spectrophotometry, and their photolysis was also studied by ^{1}H NMR spectroscopy, and one of the derivatives was used as a model 7-nitroindoline-*S*-thiocarba-

Scheme 2. One-Pot Two-Reaction Synthesis of Three Photoreactive 7-Nitroindoline-*S*-thiocarbamates (7, 8, and 9) and Their Photolysis to Nitrosoindoline 10 and Its Dimeric Forms, and the Corresponding Disulfides 11, 12, and 13

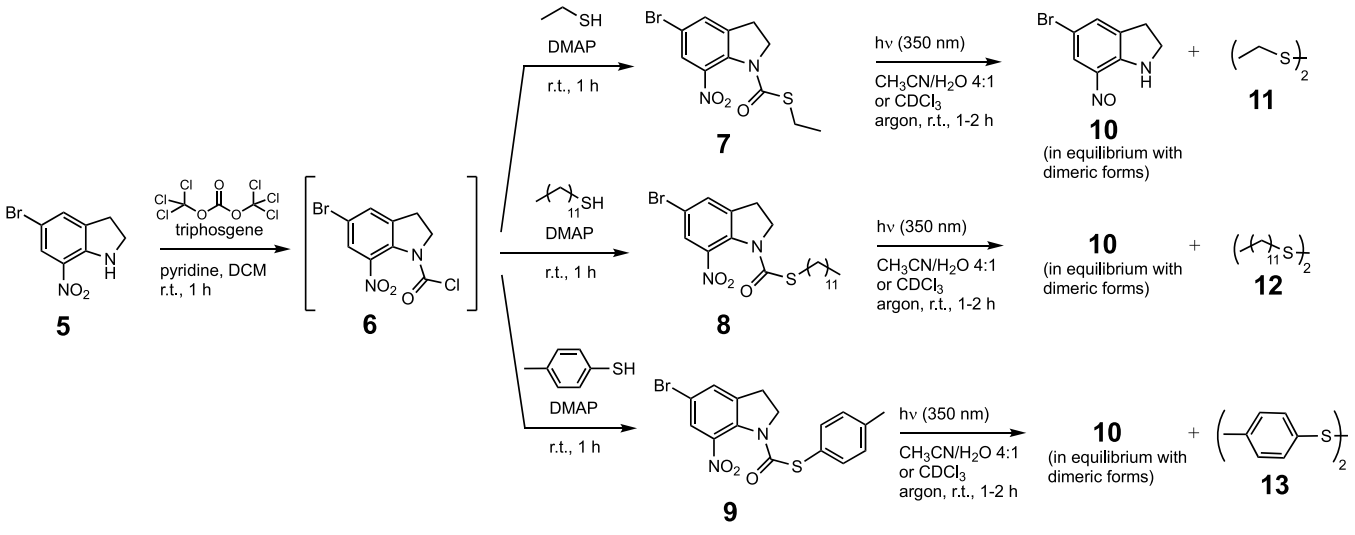

https://doi.org/10.1021/acsomega.2c08184
ACS Omega 2023, 8, 9486−9498

mate to propose a photolysis mechanism supported by *ab initio* calculations, and to study its capability to undergo photolysis by a two-photon absorption process.

RESULTS AND DISCUSSION

With the intention to generate novel, easily accessible, photoreactive compounds, commercially available 5-bromo-7-nitroindoline (**5**) was converted to carbamoyl chloride **6** *in situ* with triphosgene,[24] and further reacted with thiols to produce 5-bromo-7-nitroindoline-*S*-thiocarbamates **7**–**9** in a convenient and high-yielding (>90%) one-pot two-reaction sequence (Scheme 2). In comparison, *N*-acyl-7-nitroindolines (**1**) are often synthesized from nitroindolines (**3**) and *in situ*-generated acid chlorides.[12] In our experience, the yields of the latter syntheses can vary significantly, most likely due to difficulties in forming the acid chlorides efficiently or their partial decomposition.[14,19]

To obtain information on the photoreactivity of 7-nitroindoline-*S*-thiocarbamates, compounds **7**–**9** were illuminated with 350 nm light in a Rayonet photoreactor in CH_3CN/H_2O 4:1, and their photolysis was monitored by UV–vis spectrophotometry (Figure 1). Instead of a pure organic solvent, an aqueous/organic solvent mixture was chosen for these photolysis experiments because of the potential future applications of nitroindoline–thiocarbamates involving biomolecules and to also ensure their complete solubility. Thiocarbamates **7**, **8**, and **9** have absorption maxima at 359, 352, and 346 nm, respectively. The overlaid UV–vis spectra recorded at different time intervals during the photolysis indicate that each thiocarbamate was converted into a new aromatic compound that is detectable as a pink spot on TLC under ambient light (Figure S20). Figure 1 shows that all three thiocarbamates were consumed upon prolonged illumination, as the starting materials' absorption maxima near 350 nm disappeared, while a new absorption maximum at approximately 480 nm appeared. The photolysis of thiocarbamates **7**, **8**, and **9** has isosbestic points at 329 and 396; 326 and 396; and 329 and 395 nm, respectively (Figure 1), indicating clean conversions from one UV-active compound to another.

Further aspects of the photochemistry of thiocarbamates **7**, **8**, and **9** were investigated, including the characterization of the photolysis products of **7**, **8**, and **9** and the investigation of the photolysis pathway of compound **7** by computation.

To isolate the photolysis products, nitroindoline-*S*-thiocarbamates **7**, **8**, and **9** were illuminated at 350 nm in chloroform under argon at a preparative scale, which resulted in the efficient formation of an aromatic photolysis product and disulfides. Purification of the aromatic product by column chromatography on silica gel, and analysis by mass spectrometry and NMR spectroscopy revealed the formation of what was initially believed to be a single compound (**10**) in 94–97% yield. The formation of compound **10** was unexpected because, unlike *N*-acyl-7-nitroindolines (**1**), whose major photolysis products are 7-nitroindolines (**3**) or 7-nitrosoindoles (**4**), compound **10** is a 7-nitrosoindoline (Scheme 2).

Both the ^{1}H and ^{13}C NMR spectra of the putative compound **10** showed the presence of unusual features. The ^{1}H NMR spectrum measured at 25 °C showed that one of the aromatic protons gave a notably broad and downfield-shifted signal at 8.72 ppm (Figure S14). The ^{13}C NMR spectrum measured at 25 °C also showed a broad aromatic signal at 134.4 ppm (Figure S16). A temperature-dependent NMR

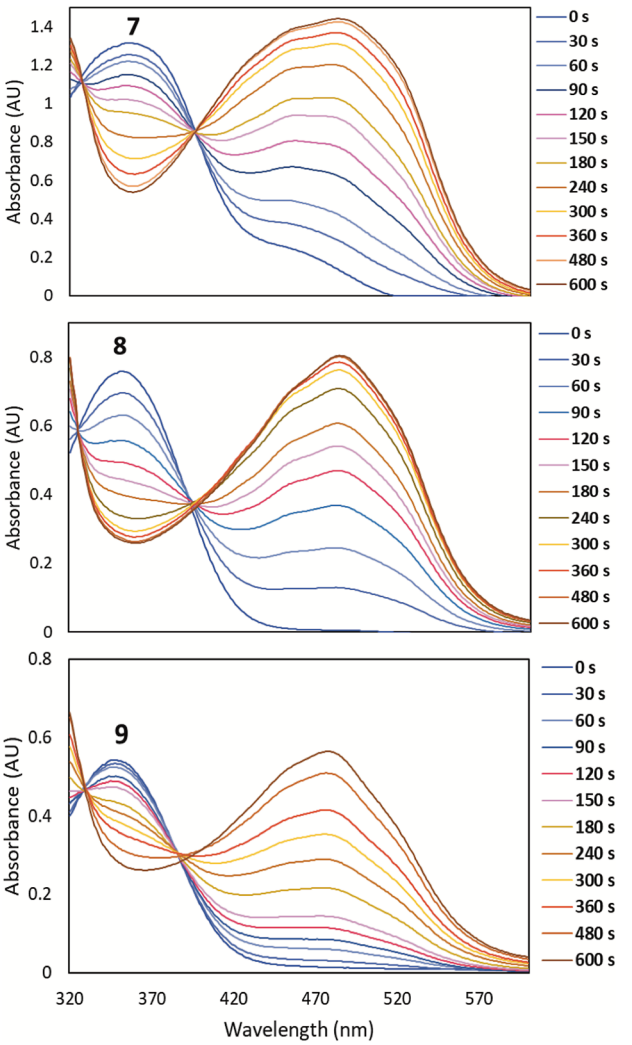

Figure 1. Photolysis of nitroindoline-*S*-thiocarbamates **7**, **8**, and **9** monitored by UV–vis spectrophotometry. The thiocarbamates were dissolved in 5 mL of acetonitrile/water = 4:1 (v/v) under argon to achieve a concentration of 0.8 mM. The photolysis was carried out under water cooling (25 °C) in a Rayonet Photochemical Chamber Reactor (RPR-200) equipped with 16 UV lamps (350 nm). In the center of the chamber, the light intensity was approximately 213 μW/cm^2. Aliquots of 100 μL were removed in time intervals, diluted with 2900 μL of the same solvent, and their UV–vis spectra were measured in 3 mL cuvettes.

study from −60 to +50 °C taken in 10 °C increments revealed that this signal sharpens at temperatures <30 and >30 °C (Figure 2).

The NMR signal shape and chemical shift dependence on temperature point toward an equilibrium between species, possibly more than two, that occurs at the NMR time scale. The exact nature of this equilibrium is difficult to discern, but other aromatic nitroso compounds similar to compound **10** have been known to form dimers with a relatively weak cis or trans azodioxy bond,[26] and the monomer/dimer equilibria have been calculated using quantum chemistry.[27] In addition, these dimers have been reported to consist of different rotamers. The rotational barriers of several meta- and para-monosubstituted, monocyclic nitrosobenzenes, as well as di- and trisubstituted derivatives, have been studied in solution by ^{1}H NMR spectroscopy.[28,29] In general, at low temperatures,

https://doi.org/10.1021/acsomega.2c08184
ACS Omega 2023, 8, 9486–9498

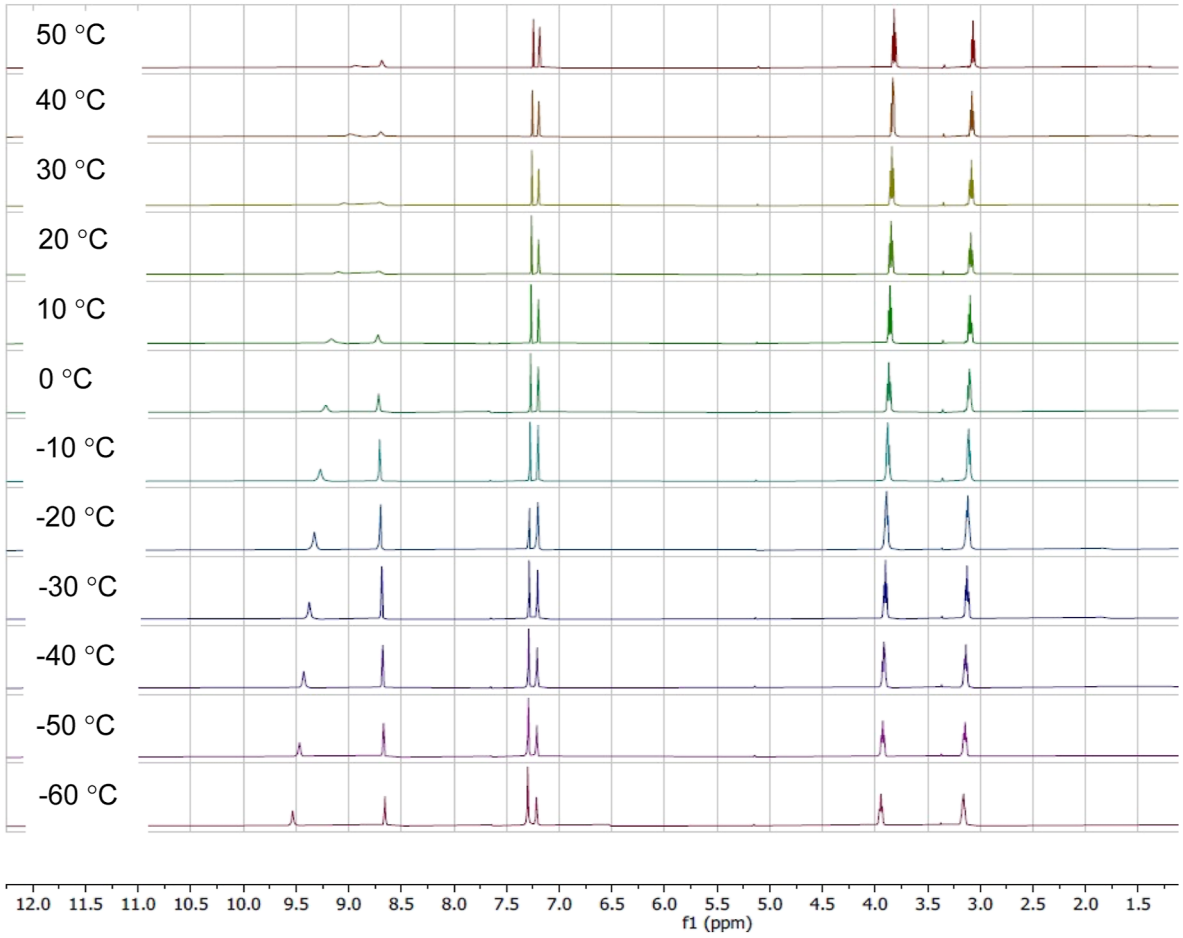

Figure 2. ^{1}H NMR spectra of photolysis product **10**, measured in $CDCl_3$ at different temperatures. The temperature-dependent broadening and sharpening of the two most downfield signals indicate equilibria of species, which are likely to involve dimers of **10**, and potentially also rotamers.

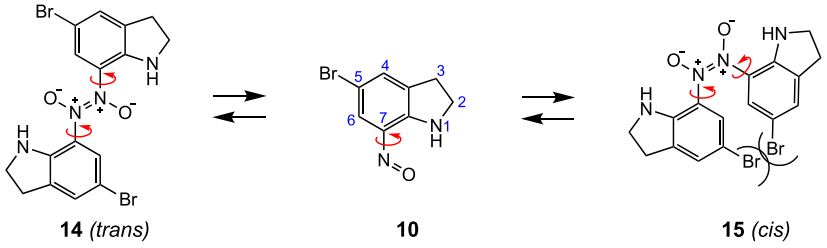

Figure 3. Nitrosoindoline **10** may dimerize by forming azodioxy species with **14** (trans) being the preferred stereoisomer over **15** (cis). Rotation about the indicated C−N bonds may also result in rotamers.

the azodioxy dimer predominated over the monomeric nitroso compounds, and in those compounds, the dimers existed mainly in the cis form with little of the trans form present. At higher temperatures, dissociation into monomeric nitrosobenzene compounds occurred. The nitroso group showed significant shielding and deshielding magnetic anisotropy, which strongly affected the hydrogens ortho to the nitroso group. Unlike the *cis*-azodioxy dimer, the trans-dimer also showed strongly deshielded aromatic protons.[28] Based on these literature reports, it is conceivable that the nitrosoindoline **10** is in equilibrium with the dimeric azodioxy forms **14** and **15** (Figure 3). However, here, B3LYP-6-31G(d,p) optimizations suggest that the trans-configured dimer **14** is preferred over the cis-configured dimer **15** by 33.2 kJ/mol due to steric interactions of the two H-6 atoms and the two bromo substituents.

In addition to cis−trans isomerization, rotation of the indoline rings about the C(7)−N bond can result in different rotamers. The ESI-ToF mass spectrum of the putative nitroso compound **10** shows that both species, monomer and dimer, are present (Figures S17 and S18), which corroborates the existence of a monomer−dimer equilibrium as reported for other aromatic nitroso compounds.[26,27] Given that ESI-ToF mass spectra are measured under high temperatures and low sample concentrations, it is not surprising that the nitroso monomer gave significantly stronger signals than the azodioxy dimer, which gave a very weak signal. Attempts to ionize the dimer at lower temperatures to produce a stronger mass spectrometric signal failed.

https://doi.org/10.1021/acsomega.2c08184
ACS Omega 2023, 8, 9486−9498

Since other nitrosoarenes show distinct ^{1}H NMR spectra for monomers and dimers, as well as the cis and trans forms of the dimers that coexist at certain temperatures,[28,29] we suspected that the major species present here are nitrosoindoline monomer **10** and trans-azodioxy dimer **14** (and possibly rotamers thereof), which are in a fast equilibrium. To shine light on the dimerization of nitrosoindoline **10**, which both NMR spectroscopy and mass spectrometry point to, computational analysis was performed. A B3LYP 6-31G(d,p) S0 ground state intrinsic reaction coordinate (IRC) solution of the dimerization of nitrosoindoline **10** to azodioxy dimer **14** is shown in Figure 4, along with the vertical S1 Tamm-Dancoff approach (TDA) results. The IRC begins from a **10**−**10** close contact dimer and proceeds through an activation barrier of 15.3 kcal/mol (64.1 kJ/mol). The reaction to form **14** is endoergic by 1.66 kcal/mol (6.94 kJ/mol). The vertical S1 TDA does not suggest a photochemical path. The N−N distance in dimer **14** is 1.332 Å, and natural bond orbital (NBO) analysis supports the presence of σ and π bonds. Rotation around this bond is likely not facile in the ground state. NBO charges of +0.254 on N and −0.529 on O support the dominant Lewis structure as drawn in Scheme 3. The close contact dimer **10**−**10** is 0.894 kcal/mol (3.74 kJ/mol) lower in energy than two isolated monomers **10**, implying that **10**−**10** is equilibrium-favored and likely very dependent on solvent. NBO analysis of **10**−**10** reveals a second-order perturbation theory interaction of 0.56 kcal/mol between the N lone pair orbital and the N═O antibonding orbital of the neighboring molecule. There are two of these reciprocal interactions totaling 1.12 kcal/mol, and this may be the dominant influence underlying the **10**−**10** close contact. The identification of the low-energy close-contact dimer **10**−**10** and the low activation barriers to the monomers **10** as well as azidodioxy dimer **14** supports a fast equilibrium between these species and a lack of separate sets of signals in the NMR spectrum. Furthermore, when examining the structures of the three species, **10**, **10**−**10**, and **14**, the chemical shift of one aromatic proton, that is, H-6, could be more affected by this equilibrium than any of the other carbon-bound protons. Indeed, one aromatic proton appears broad in the ^{1}H NMR spectrum, and also one carbon signal in the ^{13}C NMR spectrum, while all other aromatic and aliphatic protons are sharp.

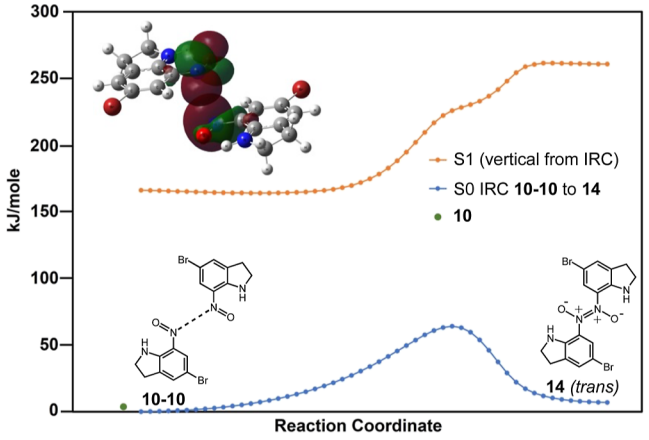

Figure 4. G09 B3LYP 6-31G(d,p) ground (S0) IRC and S1 vertical TDA results for the reaction of the close contact dimer **10**−**10** to the dimer **14**. Energies are relative to the ground state energy of the dimer **10**−**10**. The inset shows the NBO lone pair orbital of one nitroso N overlapping with the N═O π antibonding orbital of a neighboring molecule of a **10**−**10** dimer. To the left is a point depicting the energy of two isolated **10** molecules at 3.74 kJ/mol higher than **10**−**10**. The potential energy surface connecting **10** to **10**−**10** has not been calculated.

Based on the experimental and computational characterization of the photolysis products (**10**, **10**−**10**, and **14**) and additional calculations, we propose a photolytic path for *S*-ethyl-thiocarbonyl compound **7** (Scheme 3).

The S0 ground state B3LYP 6-31G(d,p) IRC was calculated for the reaction of compound **7** to (*Z*)-**16**, Figure 5. The reaction is endoergic at +27.84 kcal/mol (116.5 kJ/mol) with an activation energy of 40.45 kcal/mol (169.2 kJ/mol). The

Scheme 3. Proposed Photolysis Pathway from Nitroindoline-*S*-Thiocarbamate 7 to Nitrosoindoline 10 and Its Dimeric Forms Via a Radical Fragmentation Mechanism

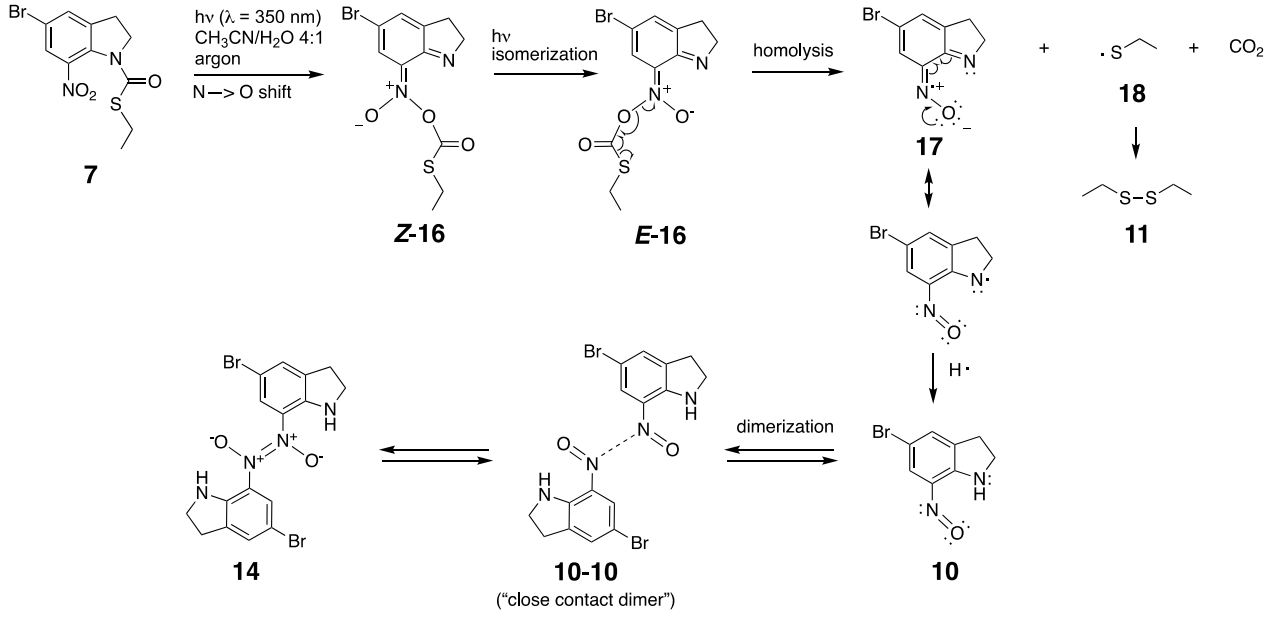

https://doi.org/10.1021/acsomega.2c08184
ACS Omega 2023, 8, 9486−9498

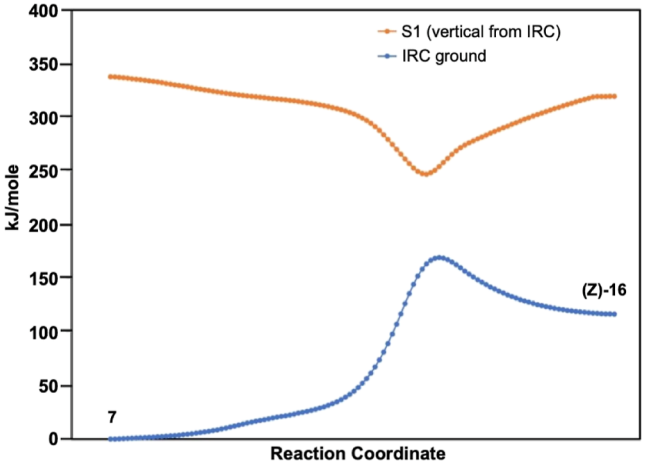

Figure 5. G09 B3LYP 6-31G(d,p) ground IRC and S1 vertical TDA results for the reaction of **7** to (*Z*)-**16**. Energies are relative to the ground-state energy of **7**.

vertical TDA calculation of the lowest singlet excited state, S1, reveals an activation-less process to a minimum near the ground state transition state, facilitating a photochemical path. Note that this finding is similar to the PM3 exploration of the acyl shift in *N*-acetyl-7-nitroindolines.[6]

We were not able to computationally locate a radical fragmentation path for (*Z*)-**16**, but there is a photochemical isomerization path to (*E*)-**16** from which a radical fragmentation path was found. The B3LYP ground IRC and vertical singlet S1 TDA for this isomerization are shown in Figure 6. The *E* isomer is favored by 1.32 kcal/mol (5.51 kJ/

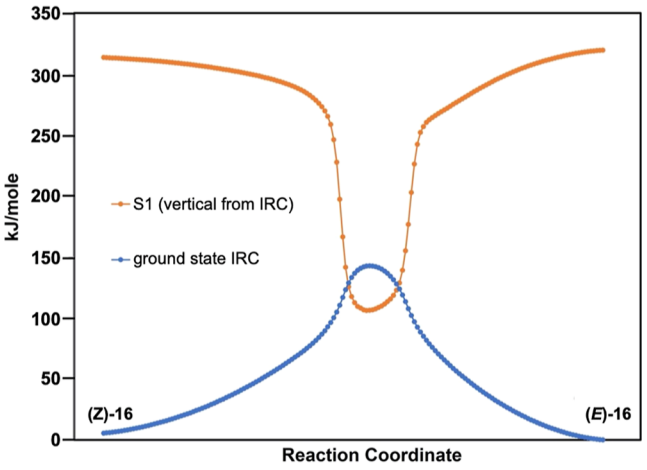

Figure 6. G09 B3LYP 6-31G(d,p) ground IRC and S1 vertical TDA results for the reaction of (*Z*)-**16** to (*E*)-**16**. Energies are relative to the ground state energy of (*E*)-**16**.

mol), with an activation from *Z* to *E* of 32.77 kcal/mol (137.2 kJ/mol). The high activation barrier may preclude a rapid ground-state interconversion. The vertical S1 can proceed by an activation-less process to cross S0 near the ground state transition state. Possibly, a conical intersection could be found by a multiconfigurational calculation, which we did not undertake. A photochemical interconversion between *Z* and *E* seems available.

The UB3LYP 6-31G(d,p) ground state IRC for the fragmentation of (*E*)-**16** is endoergic (26.83 kcal/mol; 112.24 kJ/mol) and proceeds to CO_2, resonance-stabilized radical **17**, and ethylthiyl radical **18**. The ground state activation energy is 29.38 kcal/mol (112.94 kJ/mol), Figure 7. NBO 7.0 analysis of the final ground state IRC product

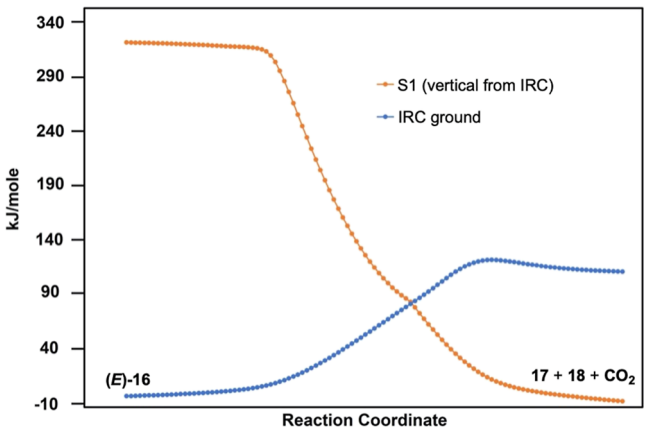

Figure 7. G09 U-B3LYP 6-31G(d,p) ground IRC and S1 vertical TDA results for the fragmentation of (*E*)-**16** into radical **17**, CO_2, and the ethylthiyl radical **18**. Energies are relative to the ground state energy of (*E*)-**16**.

structure shows S lone pair (LP) occupancies of 1.99486, 1.96200, and 1.15837. The NBO charge on S is −0.032, and the NBO charge on the EtS fragment is −0.135. This data is consistent with the EtS fragment being a radical centered on S.

A vertical TDA evaluation of the ground IRC suggests that the lowest singlet state S1 (374.89 nm; f = 0.0252) of (*E*)-**16** fragments without activation into CO_2 and the same radical products as the ground state IRC. NBO 7.0 analysis of the S1 excited state products shows S LP occupancies of 1.99518, 1.86907, and 1.13911, an NBO charge of 0.076 on S, and a net NBO charge of −0.016 on the EtS fragment. This data is consistent with a radical located on the S of EtS. The ground IRC and vertical S1 states cross at approximately 19.5 kcal/mol, suggesting a conical intersection or avoided crossing may provide a lower energy ground state path than the calculated ground state IRC. Resolving this and identifying a possible conical intersection or avoided crossing will require a multiconfigurational interaction investigation. It is possible that S1 can also be populated by internal conversion from S2 (362.79 nm), which has a larger oscillator strength of f = 0.3173.

Homolysis of the N−O bond of (*E*)-**16** is likely to occur, resulting in radicals **17** and **18**. The resonance-stabilized radical **17** may abstract a hydrogen from its surroundings to form the nitrosoindoline **10** and its dimeric forms, which are in equilibrium with each other. Recombination of the ethylthiyl radical (**18**) forms diethyl disulfide (**11**). All of the processes from **7** to **16** to **10**, **17**, and **18** appear to be pathways that can be photochemically facilitated. The equilibria between **10**, **10**−**10**, and **14** appear to be thermal. While we did not computationally identify a path of fragmentation of (*Z*)-**16**, it seems likely photochemical fragmentation should occur out of this isomer, and the isomerization to (*E*)-**16**, while likely photochemically facile, may not be necessary. It is also possible that fragmentation might occur during the photo-isomerization process.

To further experimentally corroborate the photolysis path proposed in Scheme 3, nitroindoline-thiocarbamates **7**, **8**, and

https://doi.org/10.1021/acsomega.2c08184
ACS Omega 2023, 8, 9486−9498

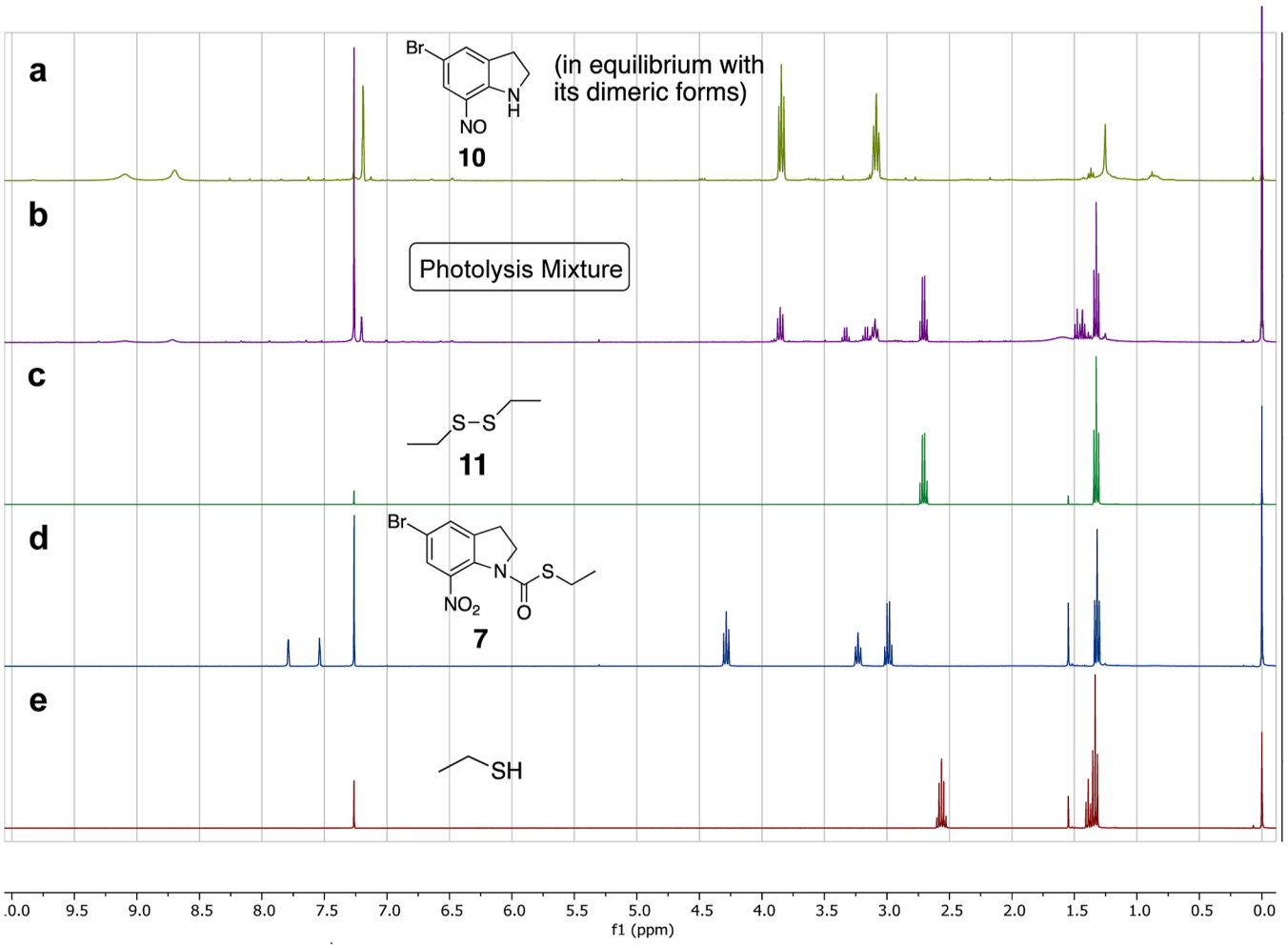

Figure 8. Comparison of ^{1}H NMR spectra in $CDCl_3$: (a) purified 7-nitrosoindoline **10** (in equilibrium with its dimeric forms); (b) photolysis reaction mixture after 1h of illumination of thiocarbamate **7** at 350 nm; (c) commercial diethyl disulfide (**11**); (d) 7-nitroindoline-*S*-thiocarbamate **7**; and (e) commercial ethanethiol.

9 dissolved in $CDCl_3$ were illuminated with light of λ = 350 nm in a Rayonet photoreactor for 2 h. Figures 8−10 show the ^{1}H NMR spectra of the thiocarbamate starting materials **7**, **8**, and **9**, their photolysis reaction mixtures, their purified photolysis product **10** (in equilibrium with its dimeric forms), and authentic, commercial disulfides and thiols, respectively. The presence of nitrosoindoline **10** (and its dimeric forms) as well as the corresponding disulfides in all three photolysis reaction mixtures supports the reaction path proposed for the photolysis of thiocarbamate **7** in Scheme 3. Figures 8−10 show that in all three photolysis reaction mixtures (Figures 8b, 9b, and 10b) the thiocarbamates **7**, **8**, and **9** (Figures 8d, 9d, and 10d) were completely consumed, and all three reactions produced 7-nitroindoline **10**, which is in equilibrium with its dimeric forms (Figures 8a, 9a, and 10a). Comparing the ^{1}H NMR spectra of the photolysis mixtures with the corresponding authentic disulfides (Figures 8c, 9c, and 10c) and thiols (Figures 8e, 9e, and 10e) shows that all three photolysis mixtures contain disulfides but not thiols. The photolysis reactions are not entirely clean. The crude photolysis mixture in Figure 8b shows two small triplets at 1.43 and 1.48 ppm and two small quartets at 3.16 and 3.33 ppm. These minor signals appear to stem from two ethyl groups of unknown byproducts. Likewise, the ^{1}H NMR spectrum in Figure 9b reveals two small multiplets at 2.88 and 2.77 pm among others, and the ^{1}H NMR spectrum in Figure 10b shows small signals at 2.42, 2.38, 2.33, 2.31, and 2.24 ppm of unknown minor byproducts. While the photolysis of thiocarbamates **7**, **8**, and **9** produced 7-nitrosoindoline **10** (and its dimeric forms) nearly quantitatively in 94%, 95%, and 97% isolated yield, respectively, the disulfides **11**, **12**, and **13** were produced in only 60% (NMR-based), 61%, and 31% yield, respectively. However, all major ^{1}H NMR signals of the reaction mixtures (Figures 8b, 9b, and 10b) are consistent with the proposed radical fragmentation shown in Scheme 3, which depicts the major photolysis path of 7-nitroindoline-*S*-thiocarbamates. The photochemical conversion of the 7-nitroindoline-*S*-thiocarbamates **7**, **8**, and **9** to a nitrosoindoline derivative was also corroborated by FT-IR spectroscopy. The starting materials show absorptions at 1657−1676 cm^{-1} indicative of the carbonyl group, and 1536−1533 and 1360−1365 cm^{-1} indicative of the nitro group, while the product has absorptions at 3256 cm^{-1} indicative of an amine, and 1572 cm^{-1} indicative of a nitroso group (Figures S5, S9, S13, and S19).

Our results indicate that the mechanism and products of the photolysis of 7-nitroindoline thiocarbamates (Scheme 3) differ from the two photolysis pathways previously reported for the analogous 7-nitroindoline amides (Scheme 1). Interestingly,

https://doi.org/10.1021/acsomega.2c08184
ACS Omega 2023, 8, 9486−9498

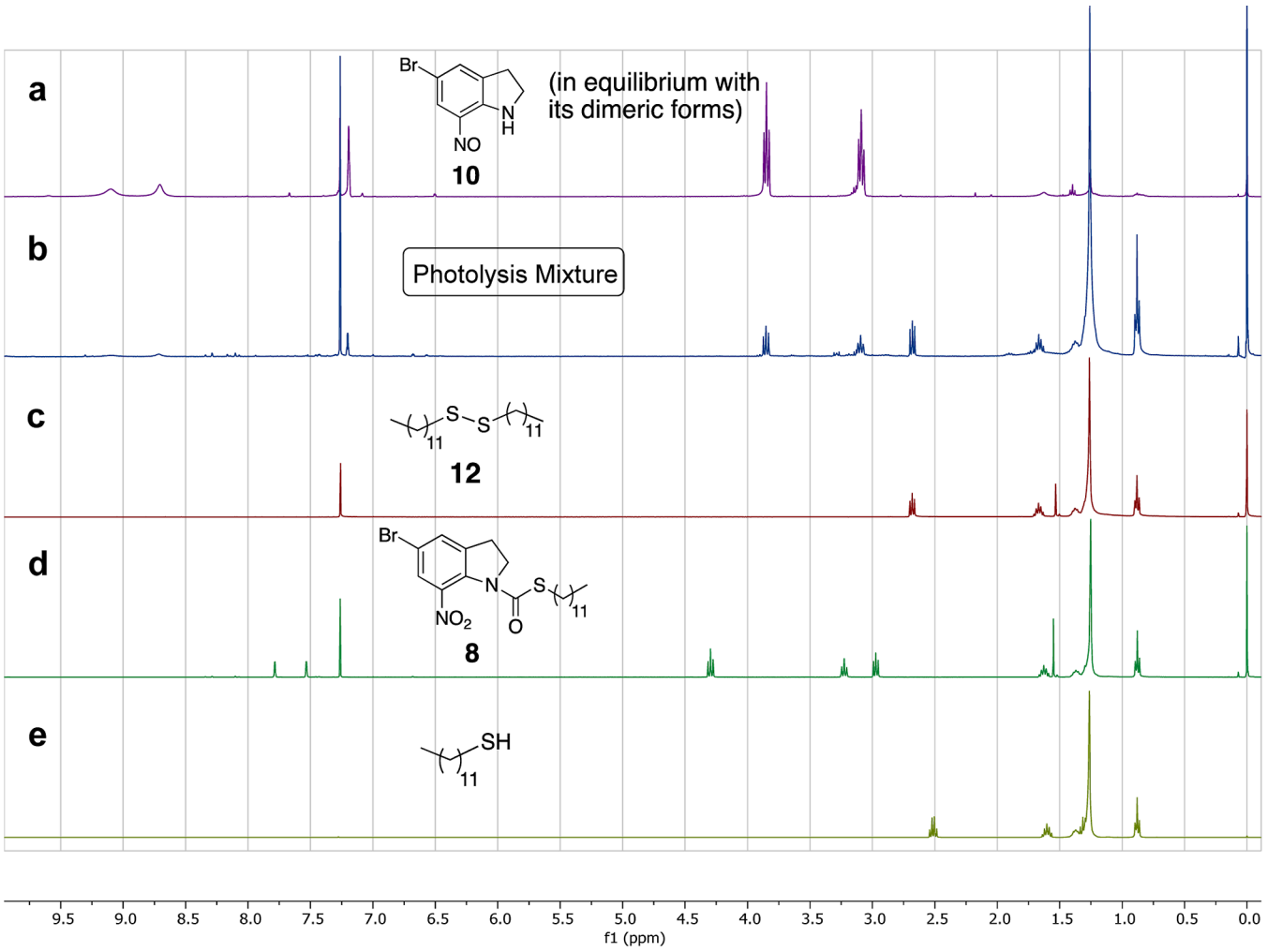

Figure 9. Comparison of ^{1}H NMR spectra in $CDCl_3$: (a) Purified 7-nitrosoindoline **10** (in equilibrium with its dimeric forms); (b) photolysis reaction mixture after 1 h of illumination of thiocarbamate **8** at 350 nm; (c) commercial didodecyl disulfide (**12**); (d) 7-nitroindoline-*S*-thiocarbamate **8**; and (e) commercial dodecaneanethiol.

when conducting photochemical reactions with *N*-acyl-7-nitroindolines in the past, we had often observed a very weak "pink spot" on TLC. Attempts to isolate this product had failed; therefore, we had not been able to characterize it. However, it cannot be excluded that the photolysis of *N*-acyl-7-nitroindolines (**1**) also produces 7-nitrosoindolines, albeit only in trace amount quantities as minor byproducts.

Two-Photon Absorption of Thiocarbamate 7. Since *N*-acyl-7-nitroindolines (**1**) are well-known for undergoing two-photon absorption using infrared femtosecond laser light,[21,22] with a two-photon cross-section large enough for biological applications,[5,8] we hypothesized that nitroindoline-*S*-thiocarbamates might show similar behavior. Like *N*-acyl-7-nitroindolines (**1**), nitroindoline-*S*-thiocarbamate **7** is fluorescent and photo-decomposed into non-fluorescent compounds [nitrosoindoline **10** and its dimeric forms **10**−**10** and **14**, CO_2, and diethyl disulfide (**11**)]. The fluorescence decay can be used to determine if a two-photon absorption process takes place indeed.

A few μg of thiocarbamate **7** dissolved in DCM were spotted on a silica thin layer chromatography plate, and the solvent was evaporated. Using fluorescence microscopy, the light of a femtosecond laser (λ = 710 nm) was focused on compound **7**. The compound's fluorescence was detected with a two-photon microscope, and images were captured through a home-built software program. Each frame has 500 × 500 pixels. Each final static image was an average of 30 frames. In the two-photon photolysis experiment, a photomask was placed at the intermediate image plane in the optical path, and a square pattern was projected onto the objective lens focal plane to partially block the illumination light for pattern formation. The fluorescence decay was measured at different locations on the TLC plate with pristine (undecomposed) thiocarbamate **7**. The images of one representative location before and after laser illumination are shown in Figure 11. The square shape in the right image corresponds to the area where femtosecond laser light was allowed through, thus thiocarbamate **7** had decomposed and no longer fluoresced. This is qualitative evidence that two-photon absorption photolysis of nitroindoline-*S*-thiocarbamates does, in fact, take place.

We further studied the fluorescence decay process under various laser powers, where the decay dynamics are getting faster with increasing powers (Figure 12). This decay process shows exponential behavior (red fitting curves), indicating photo absorption induced fluorescence decay. The exponential decay constant β versus laser power is plotted in the log−log graph as shown in Figure 13. In two-photon absorption processes, the absorption rate is proportional to the square of

https://doi.org/10.1021/acsomega.2c08184
ACS Omega 2023, 8, 9486−9498

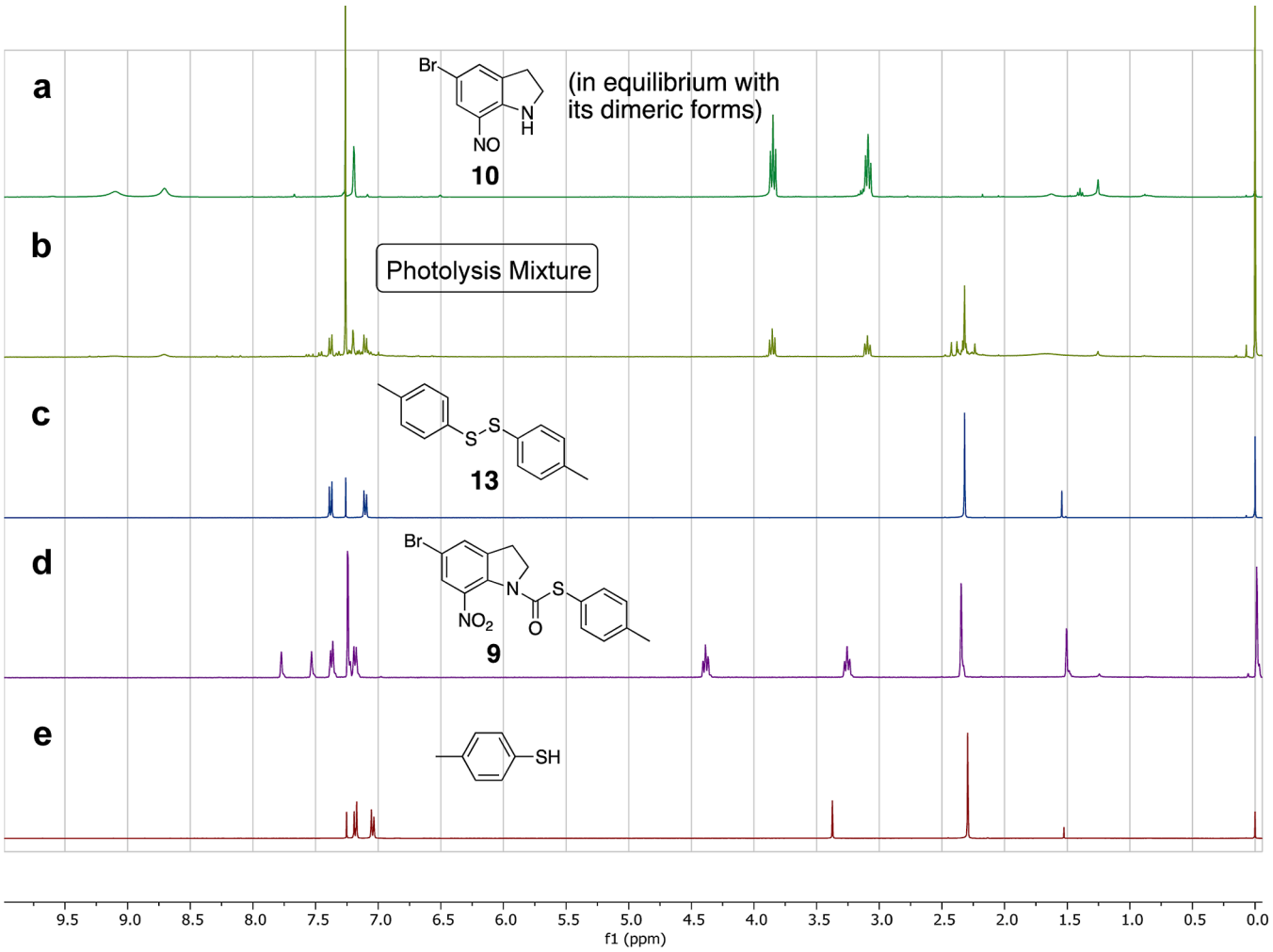

Figure 10. Comparison of ^{1}H NMR spectra in $CDCl_3$: (a) purified 7-nitrosoindoline **10** (in equilibrium with its dimeric forms); (b) photolysis reaction mixture after 1 h of illumination of thiocarbamate **9** at 350 nm; (c) commercial thiocresol disulfide (**13**); (d) 7-nitroindoline-*S*-thiocarbamate **9**; and (e) commercial thiocresol.

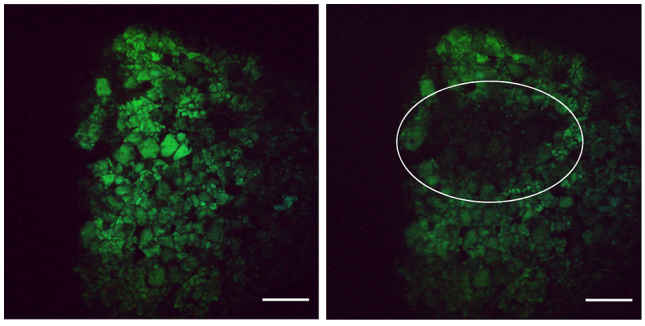

Figure 11. Fluorescent microscopic image of thiocarbamate **7** on the surface of a silica TLC plate. Left: Visualization of the fluorescence at t = 0. Right: Visualization of the fluorescence decay after 1 h of exposure only at a specific region in the center (white circle), with the pristine, non-decomposed, fluorescent material around the irradiated spot. Scale bar: 50 μm.

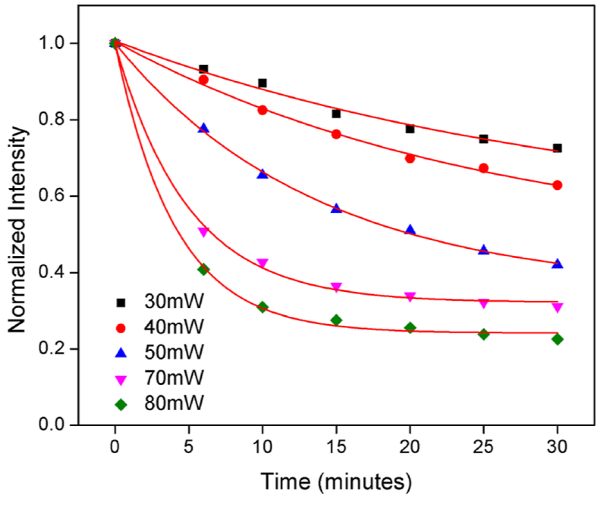

Figure 12. Fluorescence decay curves of 5-bromo-7-nitroindoline-(*S*-ethyl)-thiocarbamate (**7**) at different laser powers.

the laser intensity. Hence, this decay constant β is also proportional to the square of the laser power. In this log−log plot, theoretically, a linear curve fitting should have a slope of 2. The slope of the fitting result here is 2.2, which is close to the theoretical prediction.

The synthetic, photochemical, and photophysical insights gained by studying three 7-nitroindoline-S-thiocarbamates (**7**, **8**, and **9**), and the more in-depth characterization of the photolysis of model compound **7**, provide a foundation for

https://doi.org/10.1021/acsomega.2c08184
ACS Omega 2023, 8, 9486−9498

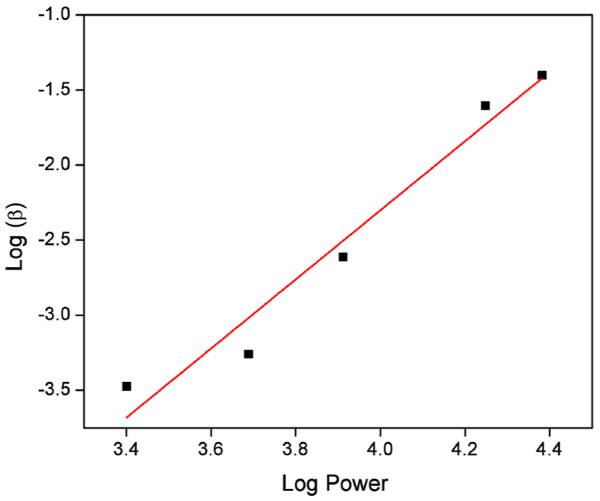

Figure 13. Double-log plot of β (fluorescence decay constant) versus laser power [mW].

exploring potential applications for this class of compounds. For example, 7-nitroindoline-*S*-thiocarbamates could be useful in synthetic organic and bioorganic chemistry, as well as materials science, where derivatization of a thiol functionality and subsequent photocleavability under neutral conditions are desired. Our data lend strong support to the capability of 7-nitroindoline thiocarbamates to undergo photolytic cleavage not only by a one-photon absorption mechanism but also by a two-photon absorption mechanism in a thin layer of material, similar to 7-nitroindoline amides (**1**).[21,22] Therefore, 7-nitroindoline thiocarbamates can potentially be utilized for micropatterning and photolithography applications using an infrared femtosecond laser, where precise spatiotemporal control is needed.

CONCLUSIONS

Here we have developed a simple, high-yield synthesis of 7-nitroindoline thiocarbamates, a new group of photoreactive compounds, and studied their photolysis. The photoreactivity of one representative of this class of compounds, that is, 5-bromo-7-nitroindoline-(*S*-ethyl)-thiocarbamate (**7**), was studied in more detail both by one-photon and two-photon absorption mechanisms. Surprisingly, the photolysis path and products differ from those of *N*-acyl-7-nitroindolines. The photolysis product, 5-bromo-7-nitrosoindoline, and its dimeric forms, as well as disulfides, were characterized by NMR spectroscopy. Both the monomeric and dimeric species of 5-bromo-7-nitrosoindoline are in equilibrium, which was confirmed by mass spectrometry and quantum chemistry. Supported by experimental and theoretical data, we were able to propose a radical fragmentation mechanism for the photolysis of 7-nitroindoline thiocarbamates. These findings expand the scope of 7-nitroindoline-containing compounds and inform the development of novel compounds and materials for photolysis applications under neutral conditions.

METHODS

Reagents, Solvents, and Materials. All chemicals were purchased as reagent grade from Thermo Fisher Scientific, Sigma-Aldrich, or Acros Organic and used without further purification. The ACS-grade solvents used for reactions were obtained from Thermo Fisher Scientific, and they were distilled using the appropriate drying agents. Reactions were performed under an argon atmosphere and under anhydrous conditions unless otherwise indicated and monitored by TLC on silica gel 60 F254 plates from EMD Millipore or Dynamic Adsorbents, Inc. Spots were detected under UV light (254 nm). The purification of the photolysis product was performed by flash column chromatography on silica gel (40−60 μm) from Thermo Fisher Scientific.

Instrumentation. ^{1}H and ^{13}C NMR spectra were recorded on a Bruker Avance III HD 400 MHz NMR spectrometer at 400 and 101 MHz or a JEOL 600 MHz NMR spectrometer at 600 MHz, respectively. Chemical shifts (in ppm) were determined relative to tetramethylsilane (δ 0.00 ppm) used as an internal standard in $CDCl_3$. Coupling constant(s) [Hz] were measured from one-dimensional ^{1}H NMR spectra. ^{1}H NMR signals were assigned by 1D spectra. MS analyses were performed on a high-resolution JEOL AccuTOF mass spectrometer using an electrospray ionization (ESI) source. The one-photon absorption photolysis reactions were performed in a Rayonet RPR200 photochemical reactor (Southern New England Ultraviolet Company, Branford, CT) equipped with 16 UV lamps (350 nm, 14 W each). UV−vis absorption spectra were measured on a Shimadzu UV-3101PC UV−vis−NIR scanning spectrophotometer using quartz cuvettes of 1 cm path length. FT-IR spectra were measured with a Thermo Scientific Nicolet iS5 FTIR spectrometer.

Laser Setup. We have utilized a custom-built video-rate microscope to perform the two-photon photocleavage experiments. Details of this microscope have been reported.[30] A femtosecond Ti/Sapphire laser (Maitai HP, 690−1040 nm, 100 fs, 80 MHz, Spectra-Physics, USA) operating at 710 nm was used for two-photon excitation of nitroindoline-*S*-ethyl-thiocarbamate **7**. A home-built raster scanner was used to scan the laser beam at 30 frames/s for two-dimensional imaging. The laser power at the focal plane was controlled by a half-wave plate and a polarizer. Upon two-photon excitation, the sample emitted fluorescent signals, which were detected by photomultiplier tubes (PMTs, R3896, Hamamatsu, USA). There were three detection channels with bandpass filters from Semrock USA: red (570−616 nm), green (500−550 nm), and blue (417−477 nm). The outputs from these three PMTs were acquired by a frame grabber (Solios eA/XA, Matrox, Quebec, Canada) to form two-dimensional R/G/B images. Each image had 500 × 500 pixels. The final image was an average of 30 consecutive images.

Synthesis of 5-Bromo-7-nitroindoline-(*S*-ethyl)-thiocarbamate (7). In a round bottom flask, commercially available 5-bromo-7-nitroindoline (**5**) (0.411 mmol) was dissolved in anhydrous DCM (2.0 mL) under argon. The yellow-orange solution was cooled to 0 °C, followed by the addition of anhydrous pyridine (1.234 mmol, 0.100 mL) and triphosgene (0.206 mmol, 0.061 g) in the dark, which resulted in a color change of the solution to pale yellow. The reaction was allowed to warm to r.t. and was monitored by TLC until the starting material **5** was completely consumed (1 h) and the carbamoyl chloride intermediate **6** was formed. Then, DMAP (1.234 mmol, 0.151 g) and ethanethiol (0.823 mmol, 0.059 mL) were added to the solution. Over time, the solution became darker yellow. The reaction was monitored by TLC until the carbamoyl chloride **6** was completely consumed, and a single new product appeared on TLC (1 h). DCM was removed under reduced pressure, and the remainder was

https://doi.org/10.1021/acsomega.2c08184
ACS Omega 2023, 8, 9486−9498

dissolved in ethyl acetate and washed with a 1 M HCl solution (2× 50 mL), followed by water (5× 50 mL) and brine (2× 50 mL), and dried over magnesium sulfate. Ethyl acetate was removed under reduced pressure to obtain 0.133 g of product **7** as an orange solid, with a 98% yield over two steps. Based on NMR spectroscopic analysis, no further purification was necessary. R_f = 0.33 (ethyl acetate/hexanes 1:4). mp = 114.2−115.4 °C. ^{1}H NMR (400 MHz, $CDCl_3$, 298 K): δ = 7.78 (s, 1H, H-6); 7.54 (S, 1H, H-4); 4.28 (t, 2H, ^3J = 8.0 Hz, H-2, H-2′); 3.23 (t, 2H, H-3, H-3′); 2.98 (q, 2H, J = 7.4 Hz, CH_2CH_3); 1.32 (t, 3H CH_2CH_3) ppm. ^{13}C NMR (101 MHz, $CDCl_3$, 298 K): δ = 167.7 [C═O], 140.3, 138.3, 133.9, 131.8, 125.5, 116.1 (arom.); 50.0 (C-2), 28.6 (C-3), 25.3 (CH_2CH_3), 15.2 (CH_2CH_3) ppm. HR ESI-ToF MS: m/z $[M + Na]^+$ calcd for $C_{11}H_{11}BrN_2NaO_3S$, 352.9571; obs. 352.9564. $[M + MeOH + Na]^+$ calcd. 384.9834; obs. 384.9817. FT-IR: 3085 (C_{sp_2}-H); 2963, 2924 (C_{sp_3}-H) 1657 (C═O); 1605, 1457, 1427 (C═C) (arom.); 1535 [NO_2(as)]; 1360 [NO_2(s)] cm^{-1}.

Synthesis of 5-Bromo-7-nitroindoline-(*S*-dodecyl)-thiocarbamate (8). Nitroindoline-*S*-thiocarbamate **8** was synthesized following a similar procedure as described for compound **7**. It was obtained in 93% yield over two steps. R_f = 0.58 (ethyl acetate/hexanes 1:3). mp = 66.6−67.4 °C. ^{1}H NMR (400 MHz, $CDCl_3$, 298 K): δ = 7.77 (s, 1H, H-6); 7.53 (s, 1H, H-4); 4.29 (t, 2H, ^3J = 8.2 Hz, H-2, H-2′); 3.23 (t, 2H, H-3, H-3′); 2.97 (t, 2H, ^3J = 7.3 Hz, S−CH_2); 1.62 (m, 2H S−CH_2CH_2); 1.37 (m, 2H S−$CH_2CH_2CH_2$); 1.29−1.23 (m, 16H); 0.88 (t, 3H, ^3J = 7.1 Hz, CH_3) ppm. ^{13}C NMR (101 MHz, $CDCl_3$, 298 K): δ = 166.8 (C═O), 139.3, 137.3, 133.9, 130.8, 124.5, 115.0 (arom.); 49.0 (C-2), 30.9 (C-3), 29.9, 28.7; 28.61; 28.55; 28.5; 28.3; 28.1; 27.8; 27.5; 21.7; 13.1 ppm. ESI-ToF MS: m/z $[M + Na]^+$ calcd. 493.1137; obs. 493.1601. FT-IR: 3089 (C_{sp_2}-H); 2959, 2918, 2852 (C_{sp_3}-H) 1657 (C═O); 1602, 1462, 1422 (C═C) (arom.); 1533 [NO_2, (as)]; 1364 [NO_2(s)] cm^{-1}.

Synthesis of 5-Bromo-7-nitroindoline-(*S*-*para*-methylphenyl)-thiocarbamate (9). Nitroindoline-*S*-thiocarbamate **9** was synthesized following a similar procedure as described for compound **7**. Compound **9** was obtained in 97% yield over two steps. R_f = 0.24 (ethyl acetate/hexanes 1:3). mp = 175.6−176.8 °C. ^{1}H NMR (400 MHz, $CDCl_3$, 298 K): δ = 7.78 (s, 1H, H6); 7.75 (s, 1H, H4); 7.39−7.38 (d, 2H, J = 7.9 Hz, thiocresol arom.); 7.21−7.19 (d, 2H, J = 7.9 Hz, thiocresol arom.); 4.02 (t, 2H, J = 8.1 Hz, H2, H2′); 3.27 (t, 2H, J = 8.1 HZ, H3, H3′); 2.36 (s, 3H, CH_3-Ph) ppm. ^{13}C NMR (101 MHz, CDCl3, 298 K): 166.6 (C═O); 140.3; 138.5; 135.4; 134.1; 132.0; 130.2; 125.7; 123.2; 116.4 (arom.); 50.4 (C2), 28.8 (C3), 21.5 (CH_3-Ph) ppm. HR ESI-ToF MS: m/z $[M + H]^+$ calcd. 414.9728; obs. 414.9720. FT-IR: 3078 (C_{sp_2}-H); 2920 (C_{sp_3}-H) 1676 (C═O); 1600, 1454, 1421 (C═C) (arom.); 1536 [NO_2 (as)]; 1365 [NO_2(s)] cm^{-1}.

Photolysis of Thiocarbamates Monitored by UV−Vis Spectrophotometry. The photolysis is described for thiocarbamate **7**. Thiocarbamates **8** and **9** were photolyzed following a similar procedure. Thiocarbamate **7** (1.3 mg) was dissolved in 5 mL of acetonitrile/water (4:1 v/v) under argon to achieve a concentration of 0.8 mM. The flask was placed into a Rayonet photoreactor and illuminated at λ = 350 nm at approximately 25 °C under water cooling. Aliquots were removed and spectrophotometrically measured in time intervals until the UV−vis spectrum of the mixture no longer changed. The reaction was completed within 10 min.

Preparative Photolysis of Thiocarbamate 7 to Produce 7-Nitrosoindoline 10 and Its Dimeric Forms. 7-Nitroindoline-(*S*-ethyl)-thiocarbamate **7** (50 mg, 0.15 mmol) was dissolved in 188 mL of $CHCl_3$ to achieve a final concentration of 0.8 mM. The mixture was illuminated with UV-light (λ = 350 nm) in a Rayonet photoreactor for 2 h. The solvent was evaporated under reduced pressure, and the crude product was purified by silica column chromatography (EtOAc/hexanes 1:4) to furnish a dark pink solid (**10** and its dimeric forms). (35 mg, yield: 94%), which appears as a pink spot on TLC (Figure S20). R_f = 0.18 in EtOAc/hexanes 1:4 (v/v). mp = 133.0−134.2 °C. ^{1}H NMR (400 MHz, $CDCl_3$, 298 K): δ 9.10 [br s, 1H, NH (exchangable with deuterium when treated with D_2O)]; 8.72 (br s, 1H, H6); 7.19 (s, 1H, H4), 3.85 (t, 2H, ^3J = 8.2 Hz, H2); 3.09 (t, 2H, H3) ppm. ^{13}C NMR δ (101 MHz, $CDCl_3$, 298 K): δ 155.5; 136.6; 134.4 (broad); 133.0; 107.5; 46.7 (C2), 26.4 (C3) ppm. HR ESI-ToF MS (monomer): m/z $[M + H]^+$ calcd for $C_8H_7BrN_2O$, 226.9815 (monoisotopic); obs. 226.9705. HR-ESI-MS (dimer): m/z $[M + H]^+$ calcd for $C_{16}H_{15}Br_2N_4O_2$, 452.9562 (monoisotopic); obs. 452.9578; m/z $[M + Na]^+$ calcd for $C_{16}H_{14}Br_2N_4NaO_2$, 474.9381 (monoisotopic); obs. 474.9403. FT-IR: 3256 (N−H); 3064 (C_{sp_2}-H); 2918, 2850 (C_{sp_3}-H); 1513, 1489, 1409 (C═C) (arom.); 1572 (N═O) cm^{-1}. Based on ^{1}H NMR spectroscopy (Figure S22), diethyl disulfide (**11**), not isolated, was produced in 60% conversion, next to two minor byproducts.

Preparative Photolysis of Thiocarbamate 8 to Produce 7-Nitrosoindoline 10 (and Its Dimeric Forms) and Didodecyl Disulfide (12). 7-Nitroindoline-(*S*-dodecyl)-thiocarbamate (**8**) (50 mg, 0.106 mmol) was dissolved in 188 mL of chloroform to achieve a final concentration of 0.56 mM. The mixture was illuminated with UV-light (λ = 350 nm) in a Rayonet photoreactor for 2 h. The solvent was evaporated under reduced pressure, and the crude product was purified by silica column chromatography in a gradient form pure hexanes to (EtOAc/hexanes 1:4) to furnish 23 mg (yield: 95%) of 7-nitroindoline **10** (in equilibrium with its dimeric forms) as a dark pink solid; R_f = 0.18 in EtOAc/hexanes 1:4 (v/v), see NMR and MS characterizations above. In addition, 13 mg of didodecyl disulfide (**12**) was isolated (yielding 61%) as a white solid; R_f = 0.55 in hexanes. The chemical shifts and R_f value of didodecyl disulfide (**12**) produced by photolysis matched those of authentic didodecyl disulfide (**12**) exactly.

Preparative Photolysis of Thiocarbamate 9 to Produce 7-Nitrosoindoline 10 (and Its Dimeric Forms) and Di-*para*-methylphenyl Disulfide (13). 7-Nitroindoline-(*S*-*para*-methylphenyl)-thiocarbamate (**9**) (50 mg, 0.13 mmol) was dissolved in 188 mL of chloroform to achieve a final concentration of 0.7 mM. The mixture was illuminated with UV-light (λ = 350 nm) in a Rayonet photoreactor for 2 h. The solvent was evaporated under reduced pressure, and the crude product was purified by silica column chromatography in a gradient form pure hexanes to (EtOAc/hexanes 1:4) to furnish 28 mg (yield: 97%) of 7-nitroindoline **10** (in equilibrium with its dimeric forms) as a dark pink solid; R_f = 0.18 in EtOAc/hexanes 1:4 (v/v), see NMR and MS characterizations above. In addition, 5 mg of di-*para*-methylphenyl disulfide (**13**) (31% yield) was isolated as a white solid; R_f = 0.32 in hexanes. The chemical shifts and R_f

https://doi.org/10.1021/acsomega.2c08184
ACS Omega 2023, 8, 9486−9498

value of di-*para*-methylphenyl disulfide (**13**) produced by photolysis matched those of authentic di-*para*-methylphenyl disulfide (**13**) exactly.

Photolysis of Thiocarbamates 7, 8, and 9 Monitored by ^{1}H NMR Spectroscopy. Thiocarbamates **7**, **8**, and **9** (1.5 mg) were separately dissolved in 0.5 mL $CDCl_3$ under argon and illuminated at 350 nm at 25 °C for 1 h. ^{1}H NMR spectra were measured before and after the illumination experiments. The photolysis of thiocarbamate **7** in an NMR tube was also conducted in acetonitrile-d_3/D_2O (4:1), which gave the same products, albeit the reaction appeared to be slightly less clean (data not shown).

Computational Methods. Quantum chemistry calculations were performed using Gaussian 09, Revision D.01 (Frisch, M. J. et al. Gaussian, Inc., Wallingford CT, 2013.) All calculations were B3LYP 6-31G(d,p) superfine-grid, tight convergence. Transition states were verified by vibrational frequency calculations. The TDA[31] was used to calculate vertical excited states from the ground-state IRC points. The transition state, ground state IRC, and vertical TDA calculations for the fragmentation of (*E*)-**16** into radicals were unrestricted. All other calculations were restricted. NBO calculations used NBO 7.0 [Glendening, E.D. et al. Theoretical Chemistry Institute, University of Wisconsin, Madison, WI (2018)]. Ground states are designated S0, while the first singlet excited state is designated S1.

■ ASSOCIATED CONTENT

Supporting Information

The Supporting Information is available free of charge at https://pubs.acs.org/doi/10.1021/acsomega.2c08184.

^{1}H and ^{13}C NMR spectra, mass spectra, and FT-IR spectra of compounds **7**, **8**, **9**, and **10**; image of a thin layer chromatogram of compounds **7** and **10**; ^{1}H NMR spectra of crude photolysis reaction mixtures and comparative spectra in selected chemical shift regions; and coordinates for relevant structures calculated by Gaussian 09 (PDF)

■ AUTHOR INFORMATION

Corresponding Authors

Chunqiang Li − *Department of Physics, University of Texas at El Paso, El Paso, Texas 79968, United States;* orcid.org/0000-0003-1220-1611; Email: cli@utep.edu

Carl W. Dirk − *Department of Chemistry and Biochemistry, University of Texas at El Paso, El Paso, Texas 79968, United States*; Email: cdirk@utep.edu

Katja Michael − *Department of Chemistry and Biochemistry, University of Texas at El Paso, El Paso, Texas 79968, United States;* orcid.org/0000-0001-6754-3702; Email: kmichael@utep.edu

Authors

Philip T. Baily − *Department of Chemistry and Biochemistry, University of Texas at El Paso, El Paso, Texas 79968, United States;* Present Address: The Division of Chemical Biology and Medicinal Chemistry, College of Pharmacy, The University of Texas at Austin, Austin, TX 78712, U.S.A

H. Patricio Del Castillo − *Department of Chemistry and Biochemistry, University of Texas at El Paso, El Paso, Texas 79968, United States*

Irodiel Vinales − *Department of Chemistry and Biochemistry, University of Texas at El Paso, El Paso, Texas 79968, United States;* orcid.org/0000-0002-4544-9587

Juan E. M. Urbay − *Department of Chemistry and Biochemistry, University of Texas at El Paso, El Paso, Texas 79968, United States*

Aurelio Paez − *Department of Metallurgical, Materials and Biomedical Engineering, University of Texas at El Paso, El Paso, Texas 79968, United States;* Present Address: NASA Marshall Space Flight Center, Huntsville, AL 35808, U.S.A.

Matthew R. Weaver − *Department of Physics, University of Texas at El Paso, El Paso, Texas 79968, United States;* Present Address: Department of Metallurgical, Materials and Biomedical Engineering, University of Texas at El Paso, El Paso, TX 79968, U.S.A.

Roberto Iturralde − *Department of Physics, University of Texas at El Paso, El Paso, Texas 79968, United States*

Igor L. Estevao − *Department of Biological Sciences, University of Texas at El Paso, El Paso, Texas 79968, United States;* orcid.org/0000-0003-3946-8375

Sohan R. Jankuru − *Department of Chemistry and Biochemistry, University of Texas at El Paso, El Paso, Texas 79968, United States;* orcid.org/0000-0002-3905-6488

Igor C. Almeida − *Department of Biological Sciences, University of Texas at El Paso, El Paso, Texas 79968, United States;* orcid.org/0000-0002-2443-8213

Complete contact information is available at: https://pubs.acs.org/10.1021/acsomega.2c08184

Author Contributions

‖P.T.B., H.P.D.C. have contributed equally to the work.

Notes

The authors declare no competing financial interest.

■ ACKNOWLEDGMENTS

P.T.B. was supported with a MARC scholarship (NIH 5T34GM008048 to Dr. Keith Pannell), and H.P.D.C. was supported through the ConTex program established by the University of Texas system and Mexico's National Council of Science and Technology (CONACYT). This work was also supported by the Partnership for Research and Education in Materials (PREM) Center for Energy and Biomaterials (NSF DMR-1827745 to Dr. Ramana Chintalapalle). Workstations for computations were provided by the College of Science, University of Texas at El Paso.

■ REFERENCES

(1) Amit, B.; Ben-Efraim, D. A.; Patchornik, A. Light-sensitive amides. The photosolvolysis of substituted 1-acyl-7-nitroindolines. *J. Am. Chem. Soc.* **1976**, *98*, 843.

(2) Morrison, J.; Wan, P.; Corrie, J. E. T.; Papageorgiou, G. Mechanism of photorelease of carboxylic acids from 1-acyl-7-nitroindolines in solutions of varying water contents. *Photochem. Photobiol. Sci.* **2002**, *1*, 960.

(3) Papageorgiou, G.; Ogden, D. C.; Barth, A.; Corrie, E. E. T. Photorelease of carboxylic acids from 1-acyl-7-nitroindolines in aqueous solution: rapid and efficient photorelease of L-glutamate. *J. Am. Chem. Soc.* **1999**, *121*, 6503.

(4) Cohen, A. D.; Helgen, C.; Bochet, C. G.; Toscano, J. P. The mechanism of photoinduced acylation of amines by N-acyl-5,7-dinitroindoline as determined by time-resolved infrared spectroscopy. *Org. Lett.* **2005**, *7*, 2845.

(5) Fedoryak, O. D.; Sul, J. Y.; Haydon, P. G.; Ellis-Davies, G. C. Synthesis of a caged glutamate for efficient one- and two-photon photorelease on living cells. *Chem. Commun.* **2005**, 3664.
(6) Mendez, J. E.; Westfall, N. J.; Michael, K.; Dirk, C. W. Photoreactivity of an N-acetyl-7-nitroindoline − Unraveling the Mechanism by Computation. *Trends Photochem. Photobiol.* **2012**, *14*, 75.
(7) Morgante, P.; Guruge, C.; Ouedraogo, Y. P.; Nesnas, N.; Peverati, R. Competition between cyclization and unusual Norrish type I and type II nitro-acyl migration pathways in the photouncaging of 1-acyl-7-nitroindoline revealed by computations. *Sci. Rep.* **2021**, *11*, 1396.
(8) Matsuzaki, M.; Ellis-Davies, G. C. R.; Nemoto, T.; Miyashita, Y.; Iino, M.; Kasai, H. Dendritic spine geometry is critical for AMPA receptor expression in hippocampal CA1 pyramidal neurons. *Nat. Neurosci.* **2001**, *4*, 1086.
(9) Smith, M. A.; Ellis-Davies, G. C. R.; Magee, J. C. Mechanism of the distance-dependent scaling of Schaffer collateral synapses in rat CA1 pyramidal neurons. *J. Physiol.* **2003**, *548*, 245.
(10) Pálfi, D.; Chiovini, B.; Szalay, G.; Kaszás, A.; Turi, G. F.; Katona, G.; Ábrányi-Balogh, P.; Szőri, M.; Potor, A.; et al. High efficiency two-photon uncaging coupled by the correction of spontaneous hydrolysis. *Org. Biomol. Chem.* **2018**, *16*, 1958.
(11) Goissis, G.; Erickson, B. W.; Merrifield, R. B. Synthesis of protected peptide acids and esters by photosolvolysis of 1-peptidyl-5-bromo-7-nitroindolines. *Proceedings of 5th American Peptide Symposium*, 1977; p 559.
(12) Pass, S.; Amit, B.; Patchornik, A. Racemization-free photochemical coupling of peptide segments. *J. Am. Chem. Soc.* **1981**, *103*, 7674.
(13) Vízvárdi, K.; Kreutz, C.; Davis, A. S.; Lee, V. P.; Philmus, B. J.; Simo, O.; Michael, K. Phototransamidation as a method for the synthesis of N-glycosyl asparagines. *Chem. Lett.* **2003**, *32*, 348.
(14) Simo, O.; Lee, V. P.; Davis, A. S.; Kreutz, C.; Gross, P. H.; Jones, P. R.; Michael, K. Synthesis of glycosyl amino acids by light induced coupling of photoreactive amino acids with glycosylamines and 1-C-aminomethyl glycosides. *Carbohydr. Res.* **2005**, *340*, 557.
(15) Kaneshiro, C. M.; Michael, K. A novel convergent synthesis of N-linked glycopeptides. *Angew. Chem., Int. Ed.* **2006**, *45*, 1077.
(16) Débieux, J.-L.; Bochet, C. G. The all-photochemical synthesis of an OGP(10−14) precursor. *Chem. Sci.* **2012**, *3*, 405.
(17) Débieux, J.-L.; Cosandey, A.; Helgen, C.; Bochet, C. G. Photoacylation of alcohols in neutral medium. *Eur. J. Org. Chem.* **2007**, *2007*, 2073.
(18) Nicolaou, K. C.; Safina, B. S.; Winssinger, N. A new photolabile linker for the photoactivation of carboxyl groups. *Synlett* **2001**, *2001*, 900.
(19) Hogenauer, T. J.; Wang, Q.; Sanki, A. K.; Gammon, A. J.; Chu, C. H.; Kaneshiro, C. M.; Kajihara, Y.; Michael, K. Virtually epimerization-free synthesis of peptide-α-thioesters. *Org. Biomol. Chem.* **2007**, *5*, 759.
(20) Pardo, A.; Hogenauer, T. J.; Cai, Z.; Vellucci, J. A.; Castillo, E. M.; Dirk, C. W.; Franz, A. H.; Michael, K. Efficient photochemical synthesis of peptide-α-phenylthioesters. *ChemBioChem* **2015**, *16*, 1884.
(21) Hatch, K. A.; Ornelas, A.; Williams, K. N.; Boland, T.; Michael, K.; Li, C. Photolysis of a peptide with N-peptidyl-7-nitroindoline units using two-photon absorption. *Biomed. Opt. Express* **2016**, *7*, 4654.
(22) Ornelas, A.; Williams, K. N.; Hatch, K. A.; Paez, A.; Aguilar, A. C.; Ellis, C. C.; Tasnim, N.; Ray, S.; Dirk, C. W.; et al. Synthesis and characterization of a photocleavable collagen-like peptide. *Org. Biomol. Chem.* **2018**, *16*, 1000.
(23) Kikuta, K.; Barta, J.; Taniguchi, Y.; Sasaki, S. Synthesis of Nucleoside Derivatives of N-Acetyl-7-nitroindoline, Their Incorporation into the DNA Oligomer, and Evaluation of Their Photoreactivity in the DNA/RNA Duplex. *Chem. Pharm. Bull.* **2020**, *68*, 1210.
(24) Hassner, A.; Yagudayev, D.; Pradhan, T. K.; Nudelman, A.; Amit, B. Light-sensitive protecting groups for amines and alcohols: the photosolvolysis of N-substituted 7-nitroindolines. *Synlett* **2007**, *2007*, 2405.
(25) Helgen, C.; Bochet, C. G. Photochemical protection of amines with Cbz and Fmoc groups. *J. Org. Chem.* **2003**, *68*, 2483.
(26) Beaudoin, D.; Wuest, J. D. Dimerization of Aromatic C-Nitroso Compounds. *Chem. Rev.* **2016**, *116*, 258.
(27) Varga, K.; Biljan, I.; Tomišić, V.; Mihalić, Z.; Vančik, H. Quantum Chemical Calculations of Monomer-Dimer Equilibria of Aromatic C-Nitroso Compounds. *J. Phys. Chem. A* **2018**, *122*, 2542.
(28) Fletcher, D. A.; Gowenlock, B. G.; Orrell, K. G. Structural investigations of C-nitrosobenzenes. Part 1. Solution state 1H NMR studies. *J. Chem. Soc., Perkin Trans. 2* **1997**, 2201.
(29) Fletcher, D. A.; Gowenlock, B. G.; Orrell, K. G. Structural investigations of C-nitrosobenzenes. Part 2.1 NMR studies of monomer−dimer equilibria including restricted nitroso group rotation in monomers. *J. Chem. Soc., Perkin Trans. 1* **1998**, 797.
(30) Acosta, Y.; Zhang, Q.; Rahaman, A.; Ouellet, H.; Xiao, C.; Sun, J.; Li, C. Imaging cytosolic translocation of Mycobacteria with two-photon fluorescence resonance energy transfer microscopy. *Biomed. Opt. Express* **2014**, *5*, 3990.
(31) Hirata, S.; Head-Gordon, M. Time-dependent density functional theory within the Tamm−Dancoff approximation. *Chem. Phys. Lett.* **1999**, *314*, 291.

https://doi.org/10.1021/acsomega.2c08184
ACS Omega 2023, 8, 9486−9498